Chapter 7
Medium-Scale Multi-hazard Risk Assessment of Gravitational Processes

Cees van Westen, Melanie S. Kappes, Byron Quan Luna, Simone Frigerio, Thomas Glade, and Jean-Philippe Malet

Abstract This section discusses the analysis of multi-hazards in a mountainous environment at a medium scale (1:25,000) using Geographic Information Systems. Although the term 'multi-hazards' has been used extensively in literature there are still very limited approaches to analyze the effects of more than one hazard in the same area, especially related to their interaction. The section starts with an overview of the problem of multi-hazard risk assessment, and indicates the various types of multi-hazard interactions, such as coupled events, concatenated events, and events changing the predisposing factors for other ones. An illustration is given of multi-hazards in a mountainous environment, and their interrelationships,

C. van Westen (✉)
Faculty of Geo-Information Science and Earth Observation (ITC), University of Twente, Hengelosestraat 99, NL-7514 AE Enschede, The Netherlands
e-mail: c.j.vanwesten@utwente.nl

M.S. Kappes
Geomorphic Systems and Risk Research Unit, Department of Geography and Regional Research, University of Vienna, Austria Universitätsstraße 7, AU-1010 Vienna, Austria

The World Bank, Urban, Water and Sanitation, Sustainable Development Department, 1818 H St. NW, Washington, DC 20433, USA

B. Quan Luna
Det Norske Veritas, Veritasveien 1, Høvik, Norway

S. Frigerio
Italian National Research Council – Research Institute for Geo-Hydrological Protection (CNR – IRPI), C.so Stati Uniti 4, IT-35127 Padova, Italy

T. Glade
Geomorphic Systems and Risk Research Unit, Department of Geography and Regional Research, University of Vienna, Austria Universitätsstraße 7, AU-1010 Vienna, Austria

J.-P. Malet
Institut de Physique du Globe de Strasbourg, CNRS UMR 7516, Université de Strasbourg/EOST, 5 rue René Descartes, F-67084 Strasbourg Cedex, France

T. van Asch et al. (eds.), *Mountain Risks: From Prediction to Management and Governance*, Advances in Natural and Technological Hazards Research 34,
DOI 10.1007/978-94-007-6769-0_7,

showing triggering factors (earthquakes, meteorological extremes), contributing factors, and various multi-hazard relationships. The second part of the section gives an example of a medium scale multi-hazard risk assessment for the Barcelonnette Basin (French Alps), taking into account the hazards for landslides, debris flows, rockfalls, snow avalanches and floods. Input data requirements are discussed, as well as the limitations in relation to the use of this data for initiation modeling at a catchment scale. Simple run-out modeling is used based on the energy-line approach. Problems related to the estimation of temporal and spatial probability are presented and discussed, and methods are shown for estimating the exposure, vulnerability and risk, using risk curves that expressed the range of expected losses for different return periods. The last part presents a software tool (Multi-Risk) developed for the analysis of multi-hazard risk at a medium scale.

Abbreviations

DTM Digital Terrain Model
DSM Digital Surface Model
GIS Geographic Information Systems
DSS Decision Support System

7.1 Introduction

A generally accepted definition of multi-hazard still does not exist. In practice, this term is often used to indicate all relevant hazards that are present in a specific area, while in the scientific context it frequently refers to "more than one hazard". Likewise, the terminology that is used to indicate the relations between hazards is unclear. Many authors speak of interactions (Tarvainen et al. 2006; de Pippo et al. 2008; Marzocchi et al. 2009; Zuccaro and Leone 2011; European Commission 2011), while others call them chains (Shi 2002), cascades (Delmonaco et al. 2006a; Carpignano et al. 2009; Zuccaro and Leone 2011; European Commission 2011), domino effects (Luino 2005; Delmonaco et al. 2006a; Perles Roselló and Cantarero Prados 2010; van Westen 2010; European Commission 2011), compound hazards (Alexander 2001) or coupled events (Marzocchi et al. 2009).

There are many factors that contribute to the occurrence of hazardous phenomena, which are either related to the environmental setting (topography, geomorphology, geology, soils etc.) or to anthropogenic activities (e.g. deforestation, road construction, tourism). Although these factors contribute to the occurrence of the hazardous phenomena and therefore should be taken into account in the hazard and risk assessment, they are not directly triggering the events. For these we need triggering phenomena, which can be of meteorological or geophysical origin (earthquakes, or volcanic eruptions). Figure 7.1 illustrates the complex interrelationships

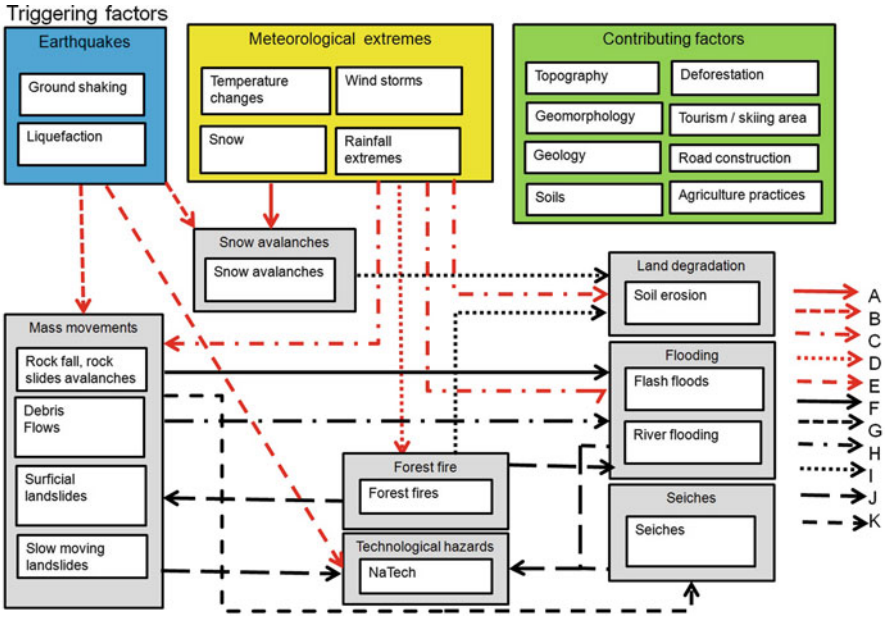

Fig. 7.1 Multi-hazard in a mountainous environment, and their interrelationships. Above the triggering factors are indicated (earthquakes, meteorological extremes), and the contributing factors. The *red arrows* indicate the hazards triggered simultaneously (coupled hazards). The *black arrows* indicate the concatenated hazards: one hazard causing another hazard over time. (**a**) Snow accumulation causing snow avalanches, (**b**) Earthquakes triggering landslides and snow avalanches simultaneously, (**c**) extreme precipitation causing landslides, debris flows, flooding and soil erosion, (**d**) drought and/or lightning causing forest fires, (**e**) earthquakes causing technological hazards, (**f**) landslides and debris flows damming rivers and causing dam break floods, (**g**) large rapid landslides or rockfalls in reservoirs causing water floods, (**h**) debris flows turning into floods in the downstream torrent section; (**i**) snow avalanches or forest fires leading to soil erosion, (**j**) forest fires leading to surficial landslides, debris flows and flash floods, (**k**) landslides, debris flows or floods leading to technological hazards

between multi-hazards potentially affecting the same mountainous environment. This graphic indicates that a multitude of different types of interrelations exists:

The first multi-hazard relationship is therefore between different hazard types that are triggered by the same triggering event. These are what we would call coupled events (Marzocchi et al. 2009). The temporal probability of occurrence of such coupled events is the same as it is linked to the probability of occurrence of the triggering mechanism. For analyzing the spatial extent of the hazard, one should take into account that when such coupled events occur in the same area and the hazard footprints overlap, the processes will interact, and therefore the hazard modeling for these events should be done simultaneously, which is still very complicated. In order to assess the risk for these multi-hazards, the consequence modeling should therefore be done using the combined hazard footprint areas, but differentiating between the intensities of the various types of hazards and using

different vulnerability-intensity relationships. When the hazard analyses are carried out separately, the consequences of the modeled scenarios cannot be simply added up, as the intensity of combined hazards may be higher than the sum of both or the same areas might be affected by both hazard types, leading to overrepresentation of the losses, and double counting. Examples of such types of coupled events is the effect of an earthquake on a snow-covered building (Lee and Rosowsky 2006) and the triggering of landslides by earthquakes occurring simultaneously with ground shaking and liquefaction (Delmonaco et al. 2006b; Marzocchi et al. 2009).

Another, frequently occurring combination are landslides, debris flows and flash-floods caused by the same extreme rainfall event. The consideration of these effects is fundamental since chains "expand the scope of affected area and exaggerate the severity of disaster" (Shi et al. 2010).

A second type of interrelations is the influence one hazard exerts on the disposition of a second peril, though without triggering it (Kappes et al. 2010). An example is the "fire-flood cycle" (Cannon and De Graff 2009): forest fires alter the susceptibility to debris flows and flash floods due to their effect on the vegetation and soil properties.

The third type of hazard relationships consists of those that occur in chains: one hazard causes the next. These are also called domino effects, or concatenated hazards. These are the most problematic types to analyze in a multi-hazard risk assessment. The temporal probability of each hazard in a chain is dependent on the temporal probability of the other hazard causing it. For example a landslide might block a river, leading to the formation of a lake, which might subsequently result in a dam break flood or debris flow. The probability of the occurrence of the flood is depending on the probability of the landslide occurring in that location with a sufficiently large volume to block the valley. The occurrence of the landslide in turn is related to the temporal probability of the triggering event. The only viable solution to approach the temporal probability of these concatenated hazards is to analyze them using Event Trees (Egli 1996; Marzocchi et al. 2009) a tool which is applied extensively in technological hazard assessment, but is still relatively new in natural hazard risk assessment. Apart from analyzing the temporal probability of concatenated events, the spatial probability is often also a challenge, as the secondary effect of one hazard (e.g. the location of damming of a river) is very site specific and difficult to predict. Therefore a number of simplified scenarios are taking into account, often using expert judgment.

7.2 Approaches for Multi-hazard Risk Assessment

Risk can be described in its simplest way as the probability of losses. The classical expression for calculating risk (R) was proposed by Varnes (1984) considered risk as the multiplication of H (Hazard probability), E (the quantification of the exposed elements at risk, and V (the vulnerability of the exposed elements at risk as the degree of loss caused by a certain intensity of the hazard).

As illustrated in Fig. 7.1 there are three important components in risk analysis: hazards, vulnerability and elements-at-risk (Van Westen et al. 2008). They are characterized by both non-spatial and spatial attributes. Hazards are characterized by their temporal probability and intensity derived from frequency magnitude analysis. Intensity expresses the severity of the hazard. The hazard component in the equation actually refers to the probability of occurrence of a hazardous phenomenon with a given intensity within a specified period of time (e.g. annual probability). Hazards also have an important spatial component, both related to the initiation of the hazard and the spreading of the hazardous phenomena (e.g. the areas affected by landslide run-out or flooding).

Elements-at-risk or 'assets' also have non-spatial and spatial characteristics (e.g. material type and number of floors for buildings). The way in which the amount of elements-at-risk is characterized (e.g. as number of buildings, number of people, economic value or the area of qualitative classes of importance) also defines the way in which the risk is presented.

The spatial interaction of elements-at-risk and hazard defines the exposure and the vulnerability of the elements-at-risk. Exposure indicates the degree to which the elements-at-risk are actually located in the path of a particular hazardous event. The spatial interaction between the elements-at-risk and the hazard footprints are depicted in a GIS by map overlaying of the hazard map with the elements-at-risk map. Physical vulnerability is evaluated as the interaction between the intensity of the hazard and the type of element-at-risk, making use of so-called vulnerability curves. For further explanations on hazard and risk assessment the reader is referred to textbooks such as Smith and Petley (2008), van Westen et al. (2009), and Alcantara-Ayala and Goudie (2010).

Loss estimation has been carried out in the insurance sector since the late 1980s using geographic information systems (GIS; Grossi et al. 2005). Since the end of the 1980s risk modelling has been developed by private companies (such as AIR Worldwide, Risk Management Solutions, EQECAT), resulting in a range of proprietary software models for catastrophe modelling for different types of hazards.

One of the first loss estimation methods that was publicly available was the RADIUS method (Risk Assessment Tools for Diagnosis of Urban Areas against Seismic Disasters), a simple tool to perform an aggregated seismic loss estimation using a simple GIS (RADIUS 1999).

The best initiative for publicly available loss estimation thus far has been HAZUS (which stands for 'Hazards U.S.') developed by the Federal Emergency Management Agency (FEMA) together with the National Institute of Building Sciences (NIBS, Buriks et al. 2004). The first version of HAZUS was released in 1997 with a seismic loss estimation focus, and was extended to multi-hazard losses in 2004, incorporating also losses from floods and windstorms (FEMA 2004). HAZUS was developed as a software tool under ArcGIS. HAZUS is considered a tool for multi-hazard risk assessment, but the losses for individual hazards are analyzed separately for earthquakes, windstorms and floods. Secondary hazards (e.g. earthquakes triggered landslides) are considered to some degree using a basic approach. Although the HAZUS methodology has been very well documented, the tool was

primarily developed for the US, and the data formats, building types, fragility curves and empirical relationships cannot be exported easily to other countries. Several other countries have adapted the HAZUS methodology to their own situation, e.g. in Taiwan (Yeh et al. 2006) and Bangladesh (Sarkar et al. 2010). The HAZUS methodology has also been the basis for the development of several other software tools for loss estimation. One of these is called SELENA (SEimic Loss EstimatioN using a logic tree Approach), developed by the International Centre for Geohazards (ICG), NORSAR (Norway) and the University of Alicante (Molina et al. 2010).

Whereas most of the above mentioned GIS-based loss estimation tools focus on the analysis of risk using a deterministic approach, the Central American Probabilistic Risk Assessment Initiative (CAPRA 2012) has a true probabilistic multi-hazard risk focus. The aim of CAPRA is to develop a system which utilizes Geographic Information Systems, Web-GIS and catastrophe models in an open platform for disaster risk assessment, which allows users from the Central American countries to analyze the risk in their areas, and be able to take informed decisions on disaster risk reduction. The methodology focuses on the development of probabilistic hazard assessment modules, for earthquakes, hurricanes, extreme rainfall, and volcanic hazards, and the hazards triggered by them, such as flooding, windstorms, landslides and tsunamis. These are based on event databases with historical and simulated events. This information is combined with elements-at-risk data focusing on buildings and population. For the classes of elements-at-risk, vulnerability data can be generated using a vulnerability module. The main product of CAPRA is a software tool, called CAPRA-SIG, which combines the hazard scenarios, elements-at-risk and vulnerability data to calculate Loss Exceedance Curves.

In New Zealand, a comparable effort is made by developing the RiskScape methodology for multi-hazard risk assessment (Reese et al. 2007; Schmidt et al. 2011). This approach aims at the provision of a generic software framework which is based on a set of standards for the relevant components of risk assessment. Another good example of multi-hazard risk assessment is the Cities project in Australia, which is coordinated by Geoscience Australia. Studies have been made for six cities of which the Perth study is the latest (Durham 2003; Jones et al. 2005). Also in Europe, several projects have developed multi-hazard loss estimations systems and approaches, such as the ARMAGEDOM system in France (Sedan and Mirgon 2003) and in Germany (Grünthal et al. 2006).

In the areas of industrial risk assessment, a number of methods have been developed using GIS-based DSSs (Decision Support Systems). One of these is the ARIPAR system (Analysis and Control of the Industrial and Harbour Risk in the Ravenna Area, Analisi e controllo dei Rischi Industriali e Portuali dell'Area di Ravenna, Egidi et al. 1995; Spadoni et al. 2000). The ARIPAR methodology is composed of three main parts: the databases, the risk calculation modules and the geographical user interface based on the Arc-View GIS environment. Currently the system is converted to ArcGIS, and also natural hazards are included in the analysis.

For risk assessment for mountainous areas, there are up to date no tools that analyze multi-hazard risk for combined processes, such as snow avalanches, rockfall, debris flows, floods and landslides. Studies on the assessment of landslide

risk or flood risk separately have been carried out, at different scales and using different methods (Bell and Glade 2004; Remondo et al. 2008; Alkema 2007; Zezere et al. 2008; Cassidy et al. 2008). However, multi-hazard risk examples are still scarce. Van Westen et al. (2002) present a case study of the city of Turrialba (Costa Rica), subjected to landslide, earthquake and flood risk, and propose three different schemes to assess hazard and vulnerability and integrate the losses afterwards. Lacasse et al. (2008) carried out a multi-hazard risk assessment related to the potential collapse of the Aknes rock slide in Norway, using an event tree, for the different scenarios which include the triggering of tsunamis. Event trees were also used by Carboni et al. (2002) to analyze the probabilities of different event scenarios of a single which might lead to the partial damming of a nearby river and the followed dambreak flooding.

When evaluating the existing methods for multi-hazard risk assessment applicable in mountainous areas, the following aspects can be mentioned:

- As many areas are exposed to more than one type of hazard, in the hazard identification phase of the risk assessment, all hazards have to be taken into account as risk analyses are spatially oriented (Greiving et al. 2006) to enable overall risk reduction.
- The models (heuristic, statistical, physically based) required for analysis of hazard for different processes vary considerably. They depend on hazard type, scale, data typology and resolution (Delmonaco et al. 2006b) and complicate the comparison of the very different results (units of the outcome, quality, uncertainty, resolution etc.) even further. A main problem is the comparability of hazards since they vary in "nature, intensity, return periods, and [. . .] effects they may have on exposed elements" (Carpignano et al. 2009).
- Also for vulnerability models a very similar situation exists. For some hazards a variety of analytical methods exist while for other processes none or only very few are established and the approaches vary widely between hazards (Hollenstein 2005).
- The way in which coupled and cascading events are evaluated. Natural hazards are not independent from each other. Instead, they are highly connected and interlinked in the natural geosystem (Kappes et al. 2010).
- The availability and quality of data are important since the model choice, the information value of the results as well as the detail of the analysis depends on these prerequisites. Each of the hazard types has different requirements with respect to the input data. The historical information on past events is crucial for most types of hazards, but the availability of historical records differs greatly among the hazard types, also depending whether these are derived from measured records (flood discharge, earthquake catalogues), archives, image interpretation, or interview (van Westen et al. 2008).
- Uncertainty plays a major role in hazard and risk assessment. The uncertainties may be due to inherent natural variability, model uncertainties and statistical uncertainties. This leads to different uncertainty levels for the various hazards. The inclusion of uncertainty is actually a necessity in probabilistic risk assessment,

and methods should still be developed to better represent these for mountain hazards and risks.

- Difficulties concerning the administrative issues as different organizations are normally involved for analyzing the hazard and risk for individual hazard types, which may make the comparison and standardization of the results difficult (Marzocchi et al. 2009). Young (2003) describes an example in the framework of environmental resources management and called this phenomenon the 'problem of interplay'.
- The natural and the administrative system are in most cases neither sharing the same spatial nor temporal framework conditions. Hazards are not restricted to administrative boundaries (e.g. river floods or earthquakes). However, hazard and risk management is mostly operating on administrative units. Therefore, a larger coordination is required between the two affected administrative units. In these cases hazard analyses should not be limited to the administrative unit, since the cause of a damaging event might be far away from the area of impact. In the case of earthquakes, for example, the impact might be far away from the epicentre. Some hazards exhibit very long return periods, therefore preventive measures will probably not show any effect during one or few legislative periods. Young (2002) entitled this phenomenon as 'problem of fit'.
- Not only the stakeholders involved in the elaboration of the analysis request detailed analysis and information. For example, the needs of emergency managers and civil protection are surely different from those of spatial planners.
- Hazard and risk assessment requires a multitude of data, coming from different data sources. Therefore it is important to have a strategy on how to make data available for risk management. Since data is coming from different organizations it is important to look at aspects such as data quality, metadata, multi-user databases, etc. Spatial risk information requires the organization of a Spatial Data Infrastructure, where through internet basic GIS data can be shared among different technical and scientific organizations involved in hazard and risk assessment.

To illustrate some of these aspects a case study is presented of medium scale multi-hazard risk assessment in the Barcelonnette area, one of the test sites within the Mountain Risk project. The Barcelonnette area is one of the best studied areas in the Alps, and a large amount of data has been collected over the years by different research teams and in different (EU funded) projects, coordinated by CNRS (Flageollet et al. 1999; Maquaire et al. 2003; Remaître 2006; Thierry et al. 2007; Malet 2010). The case study presents the results of hazard and risk assessment for floods, landslides, rockfall, snow avalanches and debris flows, based on a number of previous works (Kappes and Glade 2011; Kappes et al. 2010, 2011, 2012a, b; Bhattacharya et al. 2010a, b; Ramesh et al. 2010; van Westen et al. 2010; Hussin et al. 2012). The aim of the case study is not so much to show the actual values, as the complete multi-hazard risk analysis requires more detailed work, but more to illustrate the procedure and to show the problems involved and the levels of uncertainty.

7.3 Case Study: Medium Scale Multi-hazard and Risk Assessment in the Barcelonnette Area

The method followed in this case study closely follows the framework for multi-hazard risk assessment, presented in Fig. 7.1, with the following steps: input data collection, susceptibility assessment, hazard assessment, exposure analysis, vulnerability assessment and risk analysis. The aim of the exercise was to show the steps required for a risk assessment at the medium scale (1:25,000 to 1:50,000), and to outline the level of uncertainty associated with each of the components. Whereas risk assessment at a local scale, e.g. for a single debris flow torrent or landslide, can be done with a lower level of uncertainty, as more detailed data is available (e.g. Remaitre 2006; Hussin et al. 2012) the challenge is to do such an analysis for different types of hazards at a catchment level.

7.3.1 Input Data

The input data for the hazard and risk assessment was derived mainly from Malet (2010), and additional field investigations. A GIS database was generated, containing information on the following components: image data, topographic data, elements at risk data, environmental factors, triggering factors, and hazard inventory data (see Table 7.1). Of these factors the hazard inventory data is the most important, as it gives vital information on the dates, location, characteristics and damage caused by past occurrences.

Data from past flood events were based on technical reports, newspapers, and information from the local municipality and the RTM (Service de Restauration des Terrains de Montage– Mountain Land Restoration Service) and previous studies (Lecarpentier 1963). Data was available for one discharge station and two rainfall stations for a considerable time period (1904–2009). An inventory of active and relict landslides has been compiled by Thierry et al. (2007) at 1:10,000 scale using aerial photo-interpretation (API), fieldwork and analysis of archives. To characterize uncertainty in the mapping process, different levels of confidence were defined during the photo-interpretation and field survey (Thierry et al. 2007). A collection of historical data in archives, newspapers, monographs, technical reports, bulletins and scientific papers for the period between 1850 and 2009 has been carried out. Detailed descriptions on the type and quality of information collected and the methodologies used to analyze the data can be found in Flageollet et al. (1999) and Remaître (2006).

Over the period 1451–2010, about 600 references with exact date and location of landslide triggering have been recorded by the group of Malet (2010). For each soil slide and debris flow event, information is available on the date and location,

Table 7.1 Input data for multi-hazard risk assessment in the Barcelonnette area (OMIV 2013)

Type	Data	Characteristics
Image data	Satellite image	Downloaded from Google Earth, orthorectified, and resampled to 1.5 m pixel size
	3-D image	Anaglyph made by combining Google Earth image and DEM
	Airphotos	A set of panchromatic airphotos from different years
Topographic data	Contour lines	Digitized from topographic map, with 5 m contour interval
	DEM	Interpolated from contour lines
	Slope angle	Slope steepness made from DEM
	Slope aspect	Slope direction made from DEM
	Hillshading	Artificial illuminated made from DEM
	Openness	Visualization of DEM
	Plan curvature	Concavity-convexity made from DEM
	Flow accumulation	Contributing area made from DEM
Elements at risk data	Communes	Adm. units with population data
	Building footprints	Individual buildings & characteristics
	Cadastral map	Individual land parcels with ownership
	Roads/powerlines	Linear structures
	Bridges	Point file with bridge characteristics
	Lithology	Lithological units
Environmental factors	Materials	Unconsolidated materials
	Soils	Soil types and average depths
	Landuse 2007	Land use map of 2007
	Landuse 1980	Land use map of 1980
Triggering factors	Rainfall data	Daily rainfall for two stations from 1904 to 2009
	Discharge data	Discharge data for one station from 1904 to 2009
Hazard inventory data	Flood scenarios	Flood extend, water depth and velocity modelled for different return periods (100, 150, 250 and 500 years)
	Streams	Drainage network
	Flood events	Historical flood events from 1957 to 2008
	Avalanche field	Catalogue of avalanches mapped in field
	Avalanche photo	Catalogue mapped from airphotos
	Landslide inventory	Mapped from photos and field
	Landslide dates	Table with known landslide dates
	Heuristic hazard	Hazard map: direct mapped by experts
	Statistical hazard	Hazard map through statistical analysis by Thierry et al. (2007)
	Debris flow dates	Table with known events
	Debris flow zones	Map of catchments with DF frequency
	Rockfall area	Inventory of rockfall areas

although many of them are by approximation only. After reviewing the data, a catalogue remained of 106 mass-movement events (53 debris flows and 53 soil slides; Remaître and Malet 2011).

Information on the location of snow avalanches and rockfalls was obtained from a snow avalanche inventory made by field inventory and photo interpretation. Although a number of individual dates of occurrence could be obtained from reports, it was not possible to link the individual polygons of snow avalanches and rockfall to specific dates.

The official existing hazard map of the area is the PPR (Plan des Prévention des Risques Naturels Prévisibles, MATE/MATL 1999), which subdivides the area in three risk zones: high risk in red zones, medium risk in blue zones and low or no risk in white zones. In the red zone no permission to develop any kind of new infrastructure is allowed, whereas in the blue zone it requires a special permission.

7.3.2 Gravitational Processes Source Area Characterization

Susceptibility maps indicating the relative likelihood for the initiation of gravitational processes were generated for the various processes: snow avalanches, shallow landslides and rockfalls. Two different approaches were used: heuristic and statistical methods. The heuristic methods partly followed the methodology of the PPR (MATE/MATL 1999) by identifying sectors with homogeneous environmental characteristics, taking into account the possibility of landslide development (up- and downhill) for a 100 years period, based on a set of expert rules (Thierry et al. 2008). Shallow landslide initiation susceptibility maps for a part of the study area were also prepared using weights of evidence modelling (Thierry et al. 2007) and using fuzzy logic approach (Thiery et al. 2006) for rotational and translational landslides. In the rest of the area expert rules were used to classify specific combinations of environmental factors such as slope steepness, lithology, surface deposits, and land use. Avalanche source areas were outlined according to the methodology proposed by Maggioni (2004). Potential rock fall sources were mapped by means of a threshold slope angle and the exclusion of certain rock types as for example outcropping clays (Corominas et al. 2003). The input maps for each analysis were combined in GIS using joint-frequency tables, in which the expected susceptibility class (high, moderate, low or not susceptible) was indicated for each specific combination of the input maps. The susceptibility maps were tested using the existing inventories, and the decision rules were improved using an iterative procedure until a good agreement was reached. In order to be able to use the initiation susceptibility maps for the run-out susceptibility assessment, and given the lack of sufficient data on the dates and locations of the individual events, an assumption was introduced to indicate in which zones events were likely

Table 7.2 Assumption used in analyzing the susceptibility maps

	Triggering event		
Susceptibility class	Major event	Moderate event	Minor event
High	1	1	1
Moderate	1	1	0
Low	1	0	0
Not	0	0	0

The value of 1 indicates that gravitational processes may occur

to be initiated in three different triggering events. Table 7.2 indicates that, during a major triggering event, gravitational processes might initiate in all three zones (high, moderate and low susceptible areas). During a moderate triggering event, only gravitational processes are expected to be initiated in the moderate and high susceptible zone, and during a minor triggering event only in the high susceptible zones. Given the lack of temporal information this was the best option available. It is however, one of the major sources of uncertainty in the entire process leading to the risk assessment.

The analysis resulted in a series of 12 binary maps, indicating the presence or absence of source areas for major, moderate and minor triggering events for all types of gravitational processes.

7.3.3 Gravitational Hazard Assessment: Run-Out Modelling

The source areas defined in the previous section were subsequently used for run-out modelling on a medium (1:25,000) scale using the routing-spreading model Flow-R (Horton et al. 2008; Kappes et al. 2011). The model takes the results of the source area identification and calculates the spreading zone for each source. The choice of spreading algorithms is made by the user. This run-out modelling approach does not consider the volume of the source mass, which is another major source of uncertainty in the risk analysis. The run-out distance calculation is based on a unit energy balance, a constant loss function and a velocity threshold (Horton et al. 2008).

For each of the types of processes (debris flows, snow avalanches, rockfalls, shallow landslides) reach angles were obtained from literature (Corominas 1996). The calculation of the probable maximum run-out is based on the definition of an average slope angle between the starting and end point, considering a constant friction loss. The friction loss angles selected were between 5° and 30° and the velocity thresholds between 5 and 30 m/s depending on the type of process and the severity of the event. In the analysis a Holmgren routing algorithm was chosen for debris flows and snow avalanches because it fits reasonable with convergent flows, and the so-called D8 algorithm was used for rockfalls. The results of this analysis

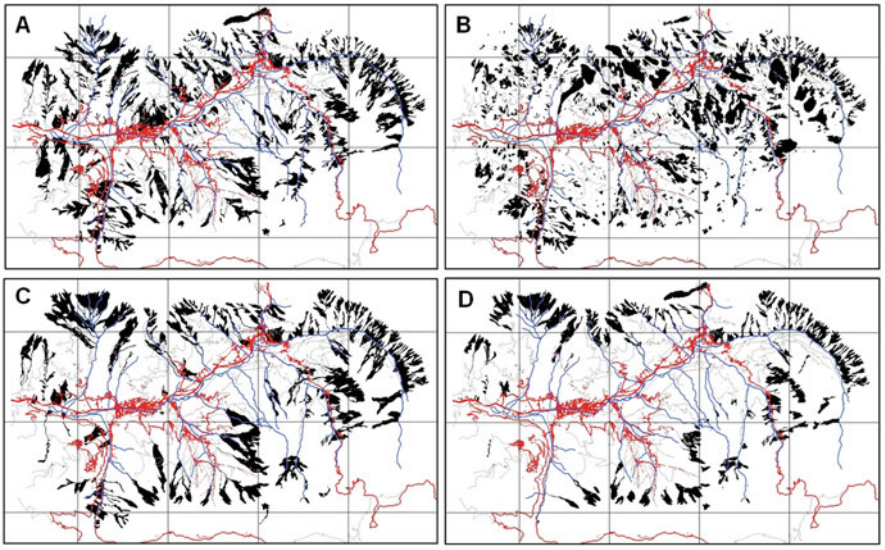

Fig. 7.2 Examples of run-out maps for major events. (**A**) Debris flow, (**B**) landslide, (**C**) rockfall and (**D**) snow avalanche

are actually more an indication rather than an accurate prediction of run-out distance and energy. Nevertheless they do give a fairly good indication as shown by Blahut (2009). Figure 7.2 shows some example of the results of the run-out assessment.

The resulting maps of Kinetic Energy were converted into impact pressure maps using average values for bulk densities of run-out materials. The maps were also classified into three susceptibility classes for run-out. It is evident from Fig. 7.4 that the determination of the source areas, and the selection of the average run-out angles may lead to an overestimation of the areas potentially affected. This process was done iteratively and the results were compared with the inventories, until a reasonable result was obtained.

7.3.4 Estimating Temporal and Spatial Probabilities of Gravitational Processes

The susceptibility assessment for gravitational processes resulted in a total of 24 susceptibility maps: three maps representing the severity classes of the triggering events (major, moderate and minor) for four hazard types (landslide, rockfall, debris flow and snow avalanche) for initiation susceptibility and a also 12 maps for the run-out susceptibility. These should be converted in hazard maps, not by changing of the actual boundaries of the susceptibility maps, but by characterizing them in terms of

Table 7.3 Summary of the information available to assess temporal, spatial and magnitude probabilities of gravitational hazards

	Spatial occurrence	Temporal information	Intensity
Snow avalanche	Only snow avalanche accumulation areas are available without dates of occurrence	Attribute tables have dates but not reliable. Return periods were estimated.	Simple estimation of impact pressure from FLOW-R Frequency-size distribution of events
Rockfall	Only rockfall accumulation areas are available without dates of occurrence	Only a few dates are known of rockfalls. Return periods were estimated	Simple estimation of impact pressure from FLOW-R
Debris flow	Only for a few of debris flows the areas are known	Debris flow dates are know for 53 events. Analysis based on antecedent rainfall analysis	Simple estimation of impact pressure from FLOW-R
Landslide	A complete landslide inventory was available for part of the area (Thierry et al. 2007). Used to calculate landslide density.	Landslide dates are known for 53 events. Analysis based on antecedent rainfall analysis	Simple estimation of impact pressure from FLOW-R Frequency-size distribution of events
Flood	Only 2 historic flood maps, and modelled flood maps for 150, 250, 500 and 1,000 year return period	Discharge information from 1905 to 2009 were analyzed using Gumbel frequency analysis	Flood depth and velocity maps are available for each return period resulting from flood modelling.

their spatial and temporal probability and intensity. The following information for each class should be indicated:

- Temporal probability: the probability that a triggering event with a severity level (major, moderate or minor) will take place within a given time period.
- Spatial probability: the probability that a pixel located within one of the susceptibility classes for the initiation and run-out susceptibility maps will actually experience a damaging gravitational process during a triggering event.
- Intensity: a measure of the intensity of the gravitational processes at a certain location, within one of the initiation or run-out susceptibility classes for the three classes of triggering events.

Ideally this process should be carried out using event-based landslide inventories, which are inventories caused by the same triggering event, for which the return period is know. Unfortunately no such event-based inventories are available for the Barcelonnette area. So the estimation was mostly based on expert opinion. Table 7.3 lists the main criteria used in the estimation of these values for the four types of gravitational processes and for flooding.

Table 7.4 Estimated return periods and uncertainties for major, moderate and minor triggering events for the four types of gravitational hazards

	Triggering event					
	Major		Moderate		Minor	
	Return period	Uncertainty estimate	Return period	Uncertainty estimate	Return period	Uncertainty estimate
Snow avalanche	150	±50	70	±25	25	±8
Rockfall	500	±200	200	±100	50	±20
Debris flow	180	±40	90	±20	30	±10
Landslide	200	±50	100	±30	40	±10

For the assessment of the temporal probability of shallow landslides and debris flows, Remaître and Malet (2011) carried out an extensive analysis of rainfall thresholds using a number of different models, such as the antecedent precipitation analysis, Intensity-Duration (I-D) model (Guzzetti et al. 2008), I-A-D model (Cepeda et al. 2009), and FLaIR (Sirangelo and Versace 2002). Based on their analysis they concluded that debris flows are triggered by storms lasting between 1 and 9 h, and are adequately predicted using an Intensity-Duration threshold, and soil slides are triggered by storms with durations between 3 and 17 h. Based on these values, an estimation could be made of the number of the return periods for triggering rainfall for debris flows and shallow landslides. For rockfalls we do not have enough known dates of occurrence to make a good frequency analysis. Based on the scarce information that we had on the occurrence of historical events, we made an estimation of the return periods, and associated levels of uncertainty of the three severity classes of triggering events for the hazard types (Table 7.4). Note that due to the lack of event-based inventories there is a very high level of uncertainty in these values. The spatial probability gives an indication of the probability that if a triggering event occurs (Major, Moderate or Minor), and an element at risk is located in the modelled run-out area, of the probability that this particular element at risk would be hit.

Since the run-out maps cover quite a large area, it is not to be expected that all the modelled areas will be affected. By analyzing the distribution of the past events, we estimated how many individual gravitational processes were initiated during a triggering event, and what their size was. We divided the modelled area of the run-out in each class by the area that was covered by gravitational processes during a similar event, to get an estimation of the spatial probability. The results are indicated in Tables 7.5 and 7.6.

Also this estimation has a considerable degree of uncertainty, as we do not have event-based landslide maps, which would allow us to directly calculate the number of gravitational processes and their average size for particular triggering events. The results also show that run-out modelling resulted in a considerable overestimation of the potentially affected areas. The better it is possible to limit the modelled run-out areas to those zones that will actually get affected, the higher the spatial probability values will be.

Table 7.5 Estimated number of gravitational processes and average sizes for major, moderate and minor triggering events for the four types of gravitational hazards

	Triggering event					
	Major		Moderate		Minor	
	Number of events	Average size (m^2)	Number of events	Average size (m^2)	Number of events	Average size (m^2)
Snow avalanche	20 ± 6	$40{,}000 \pm 10{,}000$	10 ± 3	$20{,}000 \pm 6{,}000$	5 ± 2	$10{,}000 \pm 2{,}000$
Rockfall	7 ± 4	$10{,}000 \pm 5{,}000$	5 ± 2	$5{,}000 \pm 1{,}500$	2 ± 1	$2{,}500 \pm 500$
Debris flows	15 ± 8	$40{,}000 \pm 20{,}000$	10 ± 4	$20{,}000 \pm 10{,}000$	5 ± 2	$10{,}000 \pm 2{,}000$
Landslide	50 ± 20	$10{,}000 \pm 5{,}000$	20 ± 5	$5{,}000 \pm 1{,}000$	5 ± 2	$2{,}500 \pm 500$

Table 7.6 Estimated spatial probabilities of gravitational processes for major, moderate and minor triggering events for the four types of gravitational hazards

	Triggering event		
	Major	Moderate	Minor
	Spatial probability	Spatial probability	Spatial probability
Snow avalanche	0.0305 ± 0.0168	0.0163 ± 0.0098	0.0114 ± 0.0069
Rockfall	0.0017 ± 0.0018	0.0011 ± 0.0008	0.0005 ± 0.0004
Debris flow	0.0123 ± 0.0127	0.0070 ± 0.0063	0.0069 ± 0.0041
Landslide	0.0166 ± 0.0671	0.0085 ± 0.0038	0.0025 ± 0.0015

7.3.5 Flood Hazard Assessment

The procedure for flood hazard assessment is described separately because it follows a different procedure than for gravitational processes. For analyzing the temporal probability of flood events, the flood discharge data for the period 1904–2009 was used in a statistical analysis using the Gumbel and Pearsons models to derive the relationship between discharge and return period (Bhattacharya et al. 2010a). Based on that, discharges were defined for return periods of 100, 150, 250 and 500 years. Hydraulic simulation software, in this case SOBEK and HEC-RAS, was used to analyze the flow of water in greater detail (Bhattacharya et al. 2010a; Ramesh et al. 2010). For this analysis a detailed Digital Surface Model had to be generated that incorporates all obstructions, including embankments and main buildings. This was done by interpolating the available 5 m contour lines with the incorporation of the stream network by eliminating the morphologic features within the river bed to have an un-braided structure. The building foot print layer has been used for the addition of the heights of physical elements, taking into account that there were important changes during the two historical flood events of 1957 and 2008. The changes have been incorporated and two DSM's were generated. The dyke and the embankment were included with respective heights and included in the final DSM. The land use maps from two periods were used to generate two maps of Manning's surface roughness values. For hydraulic modelling the combined 1D and 2D flood model of SOBEK was used to characterize flood events over complex topography, in both time periods, representing the situation during 1957 and during the present situation. The output data of the model consists of a series of water depth and flow velocity maps at different time steps. In this case, the maps were generated at 1 h intervals. The model also created a set of maps that summarize the simulation, which include a maximum water depth map (representing the highest water depth value that was reached at some point during the simulation), a maximum flow velocity map (representing the highest flow velocity value that was reached at some point during the simulation), and two maps that indicate the time at which the maximum water depth and the maximum flow velocity were reached and a map that shows the time at which a pixel started being inundated. To validate the flood models, the two historical flood events of 1957 and 2008 were reconstructed using the SOBEK

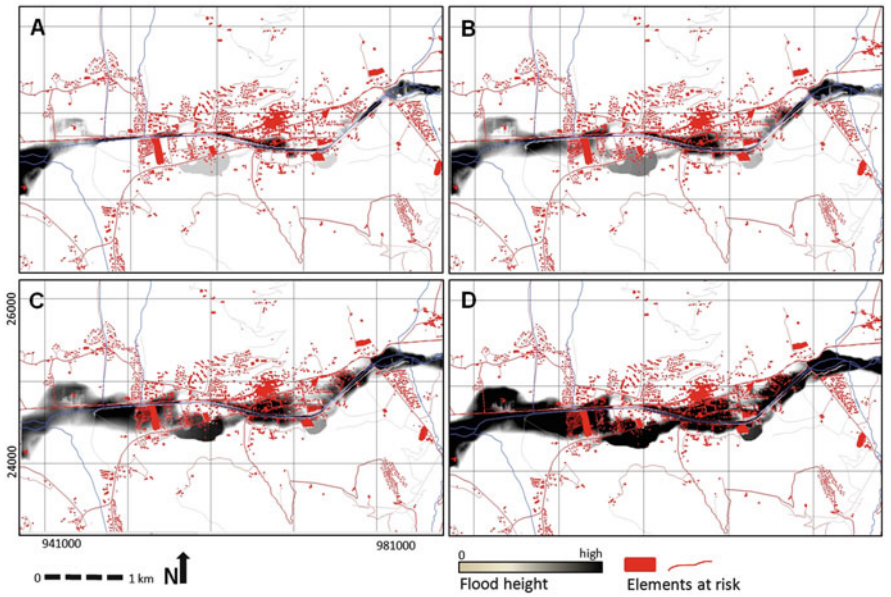

Fig. 7.3 Examples of flood maps resulting from the flood modeling for different return periods. (**A**) 150 year, (**B**) 250 year, (**C**) 500 year, (**D**) 1,000 year (Bhattacharya et al. 2010a)

modelling. The 1957 flood corresponds to a flood with a return period of 200 years. For the modelling the Digital Surface Model and the roughness map representing the 1957 situation were used (see Fig. 7.3). The analysis resulted in eight maps: maximum water height and flow velocity maps for four return periods, which can be combined in impact maps.

7.3.6 Exposure and Vulnerability Assessment

In the exposure analysis, the 24 hazard maps for the gravitational processes and the 8 maps for flood hazards were subsequently combined in GIS with the elements at risk. The building map contains information on all the buildings in the study area, where each building has its own attributes, related to building type, number of floors, occupancy type, and number of inhabitants for a daytime and night-time scenario. The exposure analysis identifies the exposed number of buildings (Table 7.7) which can also be classified according to the attributes mentioned above. The characteristics of the number of inhabitant can also be used to calculate the number of exposed people in different temporal scenarios. In this analysis also the time of the year should be incorporated, given the fact that the Barcelonnette area is a touristic destination, with a very different population distribution in winter (chalets, hotels, and ski areas), summer (camping sites, hotels and chalets) and the off season period.

Table 7.7 Summary of the number of buildings exposed to the various hazard types and severity of triggering events

	Major event	Moderate event	Minor event
Debris flow	396	171	10
Landslide	49	4	1
Rockfall	140	13	1
Snow avalanche	55	10	5
Flooding	565	364	233

Table 7.8 Exposed areas of main land use types to debris flow (in km^2)

	Major event	Moderate event	Minor event
Forest	24	4.40	3.10
Arable land	2	0.70	0.05
Pastures	12.10	4.40	0.45
Urban fabric	0.58	0.11	0.02

Table 7.9 Exposed length of main linear features to debris flows (in km)

Length affected (km)	Major event	Moderate event	Minor event
Main road	3.71	1.29	0.18
Secondary road	55.27	18.24	2.21
Unpaved road	150.41	49.01	2.91
Ski chair lift	0.12	0	0
Skilift	0.23	0	0
Electric powerline	2.33	0	0

Exposure was also calculated for land use types, by combining the recent land use maps with the 32 hazard scenarios, and representing the exposed areas of different land use types in km^2. For example, Table 7.8 shows the results for debris flows.

A similar analysis was carried out for the transportation infrastructure, and lifelines. Table 7.9 shows an example for the length of these linear features exposed to debris flows.

Minor triggering events occur mostly in uninhabited areas, and would mostly affect forested areas (e.g. debris flows, snow avalanches and rockfall). The level of uncertainty of the exposed elements at risk depends partly on the completeness (spatially and temporally) of the elements at risk map, but much more on the modeled susceptible areas. As mentioned in the previous section, the modeled run-out areas are an overrepresentation of the areas that would be actually affected in the case of a triggering event, and the variation in the spatial probability is therefore an indication of the uncertainty in the exposure.

The last component required for analyzing the risk is the physical vulnerability of the exposed elements at risk, which requires the application of vulnerability curves, giving the relation between hazard intensity and degree of damage for

different types of elements at risk. For flood vulnerability several stage-damage curves that related water height to damage were used from the UK (Pennin-Rowsell et al. 2003), Germany (Buck and Merkel 1999) and France. For the gravitational processes, several vulnerability curves and matrices were used (Bell and Glade 2004; Fuchs et al. 2007; Quan Luna et al. 2011). It should be noted here that these vulnerability curves and matrices are general approximations, and show substantial differences. For the run-out hazard maps, we use the curves derived by Quan Luna et al. (2011) that relate impact pressure to degree of damage. Given the large uncertainty of the modeled intensity of the various processes at a medium scale, and the uncertainty associated with the use of empirically derived curves, which show the average damage of a group of similar buildings exposed to the same hazard intensity, the results of the vulnerability assessment also have a very high degree of uncertainty. Furthermore, only the vulnerability of the structures was evaluated using vulnerability curves. The vulnerability in terms of building contents was evaluated by assuming a standard set of assets per building occupancy type and unit floor space, and assuming total destruction of building contents when debris flows or floods entered the ground floor.

7.3.7 Risk Assessment

The results from the previous analyses (initiation and run-out susceptibility analysis, temporal and spatial probability assessment, exposure and vulnerability analysis) were integrated in order to estimate the expected losses. The expected losses can be calculated by integrating the temporal probability of occurrence of the different scenarios and the consequences, which are calculated as the multiplication of the spatial probability, amount of exposed elements at risk and their vulnerability. The expression used for analyzing the multi-hazard risk is given by Eq. 7.1:

$$\text{Risk} = \sum_{\text{All hazards}} \left(\int_{P_T=0}^{P_T=1} P_{(T|HS)} * \left(P_{(S|HS)} * \sum \left(A_{(ER|HS)} * V_{(ER|HS)} \right) \right) \right) \tag{7.1}$$

where $P_{(T|HS)}$ is the temporal probability of a certain hazard scenario (HS); $P_{(S|HS)}$ is the spatial probability that a particular pixel in the susceptible areas is affected given a certain hazard scenario; $A_{(ER|HS)}$ is the quantification of the amount of exposed elements at risk, given a certain hazard scenario (e.g. expressed as the number or economic values) and $V_{(ER|HS)}$ is the vulnerability of elements at risk given the hazard intensity under the specific hazard scenario.

The multiplication of exposed amounts and vulnerability should be done for all elements at risk for the same hazard scenario. If the modelled hazard scenario is not expected to be producing the hazard phenomena, as is the case in most of

the gravitational processes hazard maps, the results should be multiplied with the spatial probability of hazard events $P_{(S|HS)}$. The resulting value represents the losses, which are plotted against the temporal probability of occurrence for the same hazard scenario in a so-called risk curve. This is repeated for all available hazard scenarios. At least three individual scenarios should be used, although it is preferred to use at least six events with different return periods (FEMA 2004) to better represent the risk curve. The area under the curve is then calculated by integrating all losses with their respective annual probabilities. Multi-hazard risk is calculated by adding the average annual losses for the different types of hazard. The risk analysis can be done for different spatial units. It is possible to create risk curves for the entire study area, or for administrative units (communes, census tracts) or for manually drawn homogeneous units with respect to land use.

In this study we only focused on analyzing building losses for the five different hazard types as mentioned earlier. For each hazard type we only used three hazard scenarios (major, moderate and minor) which have different return periods for each of the hazard types. We also expressed the uncertainty of each of the components of the risk assessment procedure. The results are shown in Table 7.10 and in Fig. 7.4.

The variation between the calculated losses depending on the uncertainty of the temporal probability of the identified hazard scenarios is shown in the right side of Fig. 7.4. It is clear from this figure that flood risk is much higher than any of the other four types, because it directly affects the urban center of Barcelonnette, whereas the other hazards occur more in the mountainous part of the area, where much less buildings are exposed. Debris flows follow as second important hazard type, although the expected losses are much less. When the uncertainty in terms of hazard modelling is included by incorporating also the component of spatial probability (Ps) it is clear that the expected losses for the gravitational hazards decrease considerably. The spatial probability of the modelled flood scenarios is considered one because each of the areas under the hazard footprint is expected to experience flooding, be it of different intensity. For the gravitational processes, this uncertainty is much higher, and the inclusion of the spatial probability decreases the expected losses with a factor of 100, purely based on the uncertainty of modelling the areas where actual gravitational processes are likely to happen. The better the run-out models are able to narrow down to the future sites of events, the higher the $P_{(S|HS)}$ will be. Low accuracies in modelling will therefore result in lower risks.

7.4 MultiRISK, a Platform for Multi-hazard Risk Modeling and Visualization

The calculation of multi-hazard risk requires a large number of calculation steps which could be integrated in a spatial DSS. In the framework of the Mountain Risks project a prototype software for multi-hazard risk analyses has been developed.

Table 7.10 Result of the quantitative risk assessment for the four gravitational hazards and for flood hazard

		Annual probability (P_T)		Spatial probability (P_S)		Exposed	Losses if	Expected losses (million)	
	Scenario	min	max	min	max	buildings	$P_S = 1$	min	max
Debris flow	Major	0.007	0.005	0.003	0.028	496	24.8	0.0744	1.3888
	Moderate	0.014	0.009	0.002	0.015	171	8.55	0.0171	0.2565
	Minor	0.050	0.025	0.003	0.012	10	0.50	0.0015	0.0120
Landslide	Major	0.007	0.004	0.005	0.139	49	2.45	0.0123	0.6811
	Moderate	0.014	0.008	0.005	0.013	4	0.20	0.0010	0.0052
	Minor	0.033	0.020	0.001	0.004	1	0.05	0.0001	0.0004
Rock fall	Major	0.003	0.001	0.001	0.004	240	12	0.0120	0.0960
	Moderate	0.010	0.003	0.001	0.002	13	0.65	0.0007	0.0026
	Minor	0.033	0.014	0.001	0.002	1	0.05	0.0001	0.0002
Snow avalanche	Major	0.010	0.005	0.016	0.050	55	2.75	0.0440	0.2750
	Moderate	0.022	0.011	0.008	0.027	10	0.50	0.0040	0.0270
	Minor	0.059	0.031	0.005	0.019	5	0.25	0.0013	0.0095
Flood	Major	0.001	0.001	1	1	389	100	100	160
	Moderate	0.003	0.002	1	1	357	17	17	30
	Minor	0.005	0.004	1	1	322	5	5	9

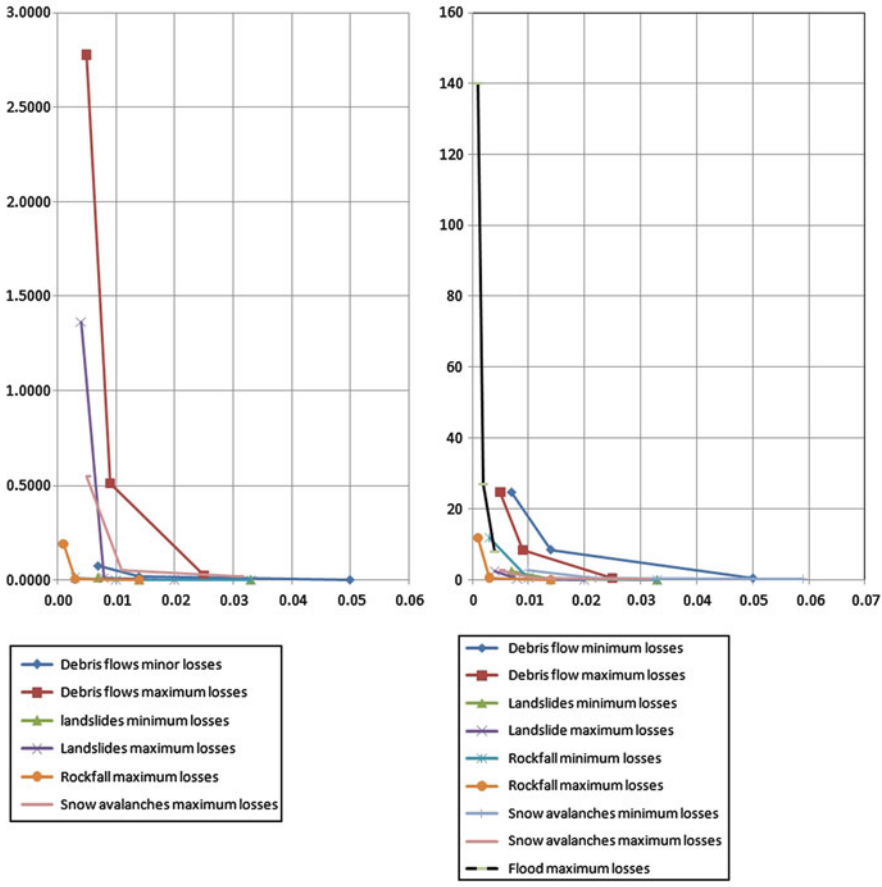

Fig. 7.4 Risk curves of the five hazard types, displaying the variation of losses (shown on X-Axis in M€) against temporal probability (annual probability shown on Y-axis). The *left graph* shows the results taking into account both temporal and spatial probability (note that the flood losses are excluded). The *right graph* shows the variation only in terms of temporal probability

This tool is designed to offer a user-friendly, fast and combined examination of multiple mountain hazards (e.g. debris flows, rock falls, shallow landslides, avalanches and river floods). Since multi-hazard studies suffer from high data requirements a top-down approach is recommendable within which, by means of a regional study, areas of potential risk and hazard interactions are identified to be subsequently analyzed in detail in local studies. The MultiRISK Modeling Tool is designed according to a top-down concept. It consists of at least two scales at which analyses are carried out – first an overview analysis and secondly detailed studies (possible extension by a third even more detailed scale for e.g. specific engineering purposes). In its current version MultiRISK consists still exclusively of the regional overview analysis (∼1:10,000–1:50,000) but will be extended in the future by

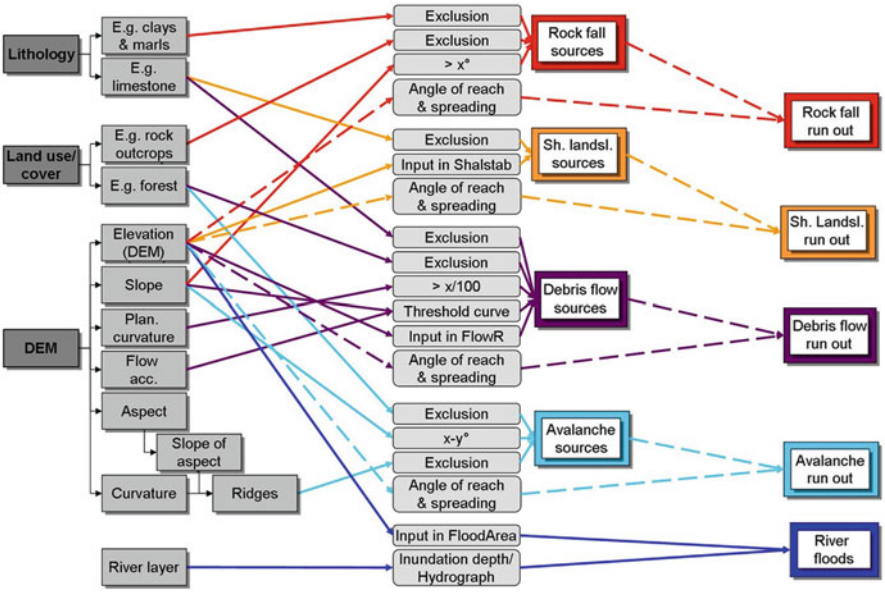

Fig. 7.5 Analysis scheme for the MultiRISK Modeling Tool (Kappes et al. 2012a, b)

local models and methods. In this section, the regional analysis scheme behind the analysis software as well as the structure of the software itself is presented shortly (for a more detailed presentation, refer to Kappes et al. 2011, 2012a, b).

For the regional analysis simple empirical models with low data-requirements were chosen. For the identification of potential rock fall sources a method was used which employs a threshold slope angle and the exclusion of certain rock types as for example outcropping clays (Corominas et al. 2003). For the flood analysis a method was selected which extrapolates the inundation over a DSM based on a fixed inundation depth (Geomer 2008). Shallow landslide source areas are modeled with Shalstab (Montgomery and Dietrich 1994), avalanche source areas are modeled according to the methodology proposed by (Maggioni 2004) and debris flow sources with Flow-R after (Horton et al. 2008). The run out of rock falls, shallow landslides, avalanches and debris flows is computed with Flow-R as described in Horton et al. (2008). The spatial input data needed for all these models is composed of a DEM and derivatives, land use/cover and lithological information. Figure 7.5 gives an indication of the decision rules used in the multi-hazard analysis.

The complexity of the analysis scheme indicates the effort necessary and the time-consumption for the step-by-step performance of the whole procedure in GIS software. Hence, an automation was undertaken to relief the modelers of the intermediate steps (Fig. 7.5), simplify the structure to the important decisions and facilitate a fast and reproducible computation and re-computation of a multi-hazard analysis (Fig. 7.6).

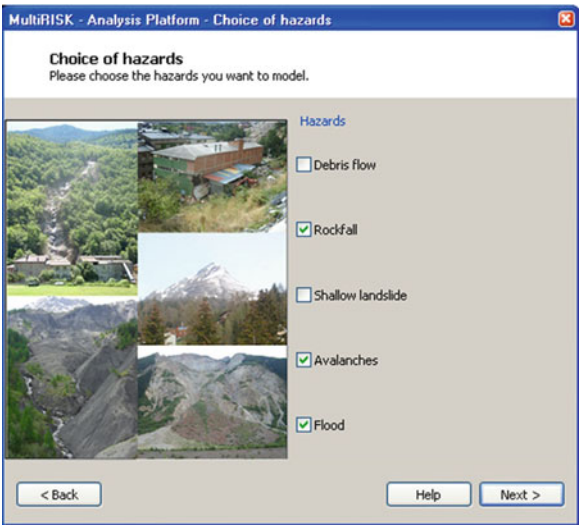

Fig. 7.6 Interface of the MultiRISK Modeling Tool

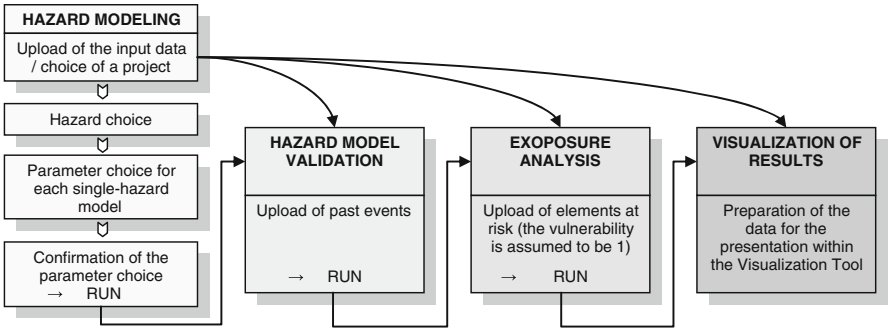

Fig. 7.7 Flow chart of the MultiRISK Modeling Tool (Kappes et al. 2012a, b)

Table 7.11 Confusion matrix (from Beguería 2006)

	Modeled	Not-modeled
Recorded	True positives	False negatives
Not-recorded	False positives	True negatives

Additionally to the hazard modeling, a model validation step as well as an exposure analysis are included (Fig. 7.7).

The validation is carried out according to Begueria (2006) by means of an overlay of the modeling result with recorded events and the area falling into the resulting four categories (Table 7.11) quantified in a confusion matrix.

The exposure analysis offered in MultiRISK is carried out by means of an overlay of the elements at risk and the single-hazard zones. The number of buildings, length of infrastructure or proportion of settled area exposed is calculated.

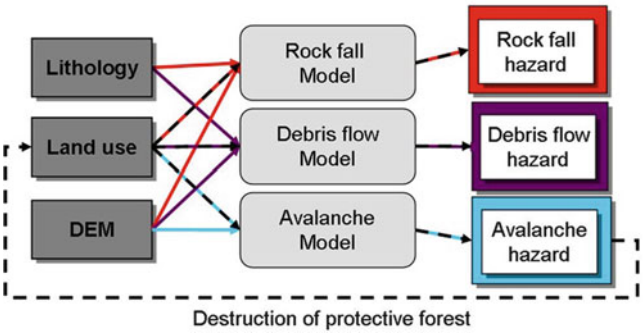

Fig. 7.8 Proposed feedback loop (From Kappes et al. 2010)

The effect of interactions is not yet implemented in the structure of the software tool but conceptual considerations how to account for them do already exist. First, it refers to the alteration of the disposition one hazard by another. Within the analysis procedure this refers to the alteration of factors which serve as input data as e.g. the impact of avalanche events on the land use (the destruction of forest) and subsequently the modification of future rock fall, debris flow and avalanche hazard this entails. By means of feedback-loops this phenomenon can be included (Fig. 7.8). The manual creation of an updated land use file for the re-upload as input file and the re-computation of the three affected hazards already allow carrying out this feedback-loop. Second, the triggering of one hazard by another resulting in so-called hazard chains has to be regarded. At a regional scale, only the identification of places potentially prone to such chains can be identified whereas their detailed examination by means of e.g. event trees is restricted to local analyses (Delmonaco et al. 2006a). Potential chains arising within the set of hazard currently included in MultiRISK are especially the undercutting of slopes during flood events and the damming of rivers and torrents due to landsliding. By an overlay of the respective hazard layers the zones can be identified.

The MultiRISK Modelling Tool is linked to the MultiRISK Visualization Tool to facilitate the display of the analysis results and together they form the MultiRISK Platform. The MultiRISK Visualization Tool is presented in Sect. 15.4.

7.5 Conclusion

This chapter outlines a number of aspects dealing with the assessment of multi-hazard risk assessment at a medium scale (1:25,000 to 1:50,000) for mountainous areas in Europe. The procedure outlined in this chapter is not intended to focus on the actual calculated risk values, as much more work needs to be done in better defining the temporal probability, in modelling the run-out areas related to hazard

events with a specific return period, in quantifying the physical vulnerability to gravitational processes, and representing the replacement costs. The main aim of this chapter was to show the procedure for quantitative multi-hazard risk assessment and to illustrate the large degree of uncertainty involved if event-based inventories are not available.

The modelling of the temporal probability of triggering events for different hazard types will remain problematic, given the limited available historical information on gravitational processes occurrences. Although this is improving nowadays as more countries are implementing national landslide inventories, often with a web-GIS interface. Also for large triggering events there are more possibilities to collect the event-based landslide inventories due to the available of more frequent and more detailed satellite data. However, the conclusion that quantitative multi-hazard risk assessment in mountainous areas can only be carried out if more detailed historic inventories are available, is too obvious. Many areas will continue to suffer from this problem, yet solutions must be found and estimations of loss should be given to improve disaster risk reduction planning. Therefore the use of tools such as the Multi-Risk platform outlined in this chapter, should be promoted, allowing for simple but efficient methods for estimating the risk of different hazards in the same area, and comparing their expected losses.

In the risk assessment a number of challenges remain. One of them is the modelling of hazard initiation points for different hazards (e.g. flooding and gravitational processes) based on the same meteorological trigger. These initiation points, which will vary with respect to the temporal probability of the triggering rainfall, should be used for modelling runout with quantifiable intensity measures. The modelling of uncertainty in this process is another major challenge, as well as the generation of vulnerability relations that incorporate uncertainties. And finally also the link with non-quantifiable aspects should be made using indicators for social, economic and environmental vulnerability.

Hazard, vulnerability and risk are dynamic, as changes occur in the hazard processes, human activities and land use/landcover patterns in mountainous areas, due to global changes. The analysis of changes in risk is therefore a very relevant topic for further study. This is the research topic of the CHANGES network (Changing Hydro-meteorological Risks – as Analyzed by a New Generation of European Scientists) funded by the EU FP7 Marie Curie Initial Training Network (ITN) Action. The project will develop an advanced understanding of how global changes (related to environmental and climate change as well as socio-economical change) will affect the temporal and spatial patterns of hydro-meteorological hazards and associated risks in Europe; how these changes can be assessed, modelled, and incorporated in sustainable risk management strategies, focusing on spatial planning, emergency preparedness and risk communication. The CHANGES network hopes to contribute to the Topical Action numbers 2 and 3 of the Hyogo Framework for Action of the UN-ISDR, as risk assessment and management, combined with innovation and education are considered essential to confront the impacts of future environmental changes (ISDR 2009). The network consists of 11

full partners and 6 associate partners of which 5 private companies, representing 10 European countries, and 12 ESR's (PhD researchers) and 3 ER's (Postdocs) are hired. The project has a duration of 4 years and has started in January 2011 (www.changes-itn.eu).

References

Alcantara-Ayala I, Goudie AS (2010) Geomorphological hazards and disaster prevention. Cambridge University Press, Cambridge

Alexander D (2001) Natural hazards. In: Encyclopedia of environmental science. Kluwer Academic Publishers, Dordrecht

Alkema D (2007) Simulating floods: on the application of a 2D-hydraullic model for flood risk assessment. International Institute for Geo-information Science and Earth Observation, Enschede

Beguería S (2006) Validation and evaluation of predictive models in hazard assessment and risk management. Nat Hazards 37:315–329

Bell R, Glade T (2004) Quantitative risk analysis for landslides – examples from Bνldudalur, NW-Iceland. Nat Hazard Earth Syst 4(1):117–131

Bhattacharya N, Kingma NC, Alkema D (2010a) Flood risk assessment of Barcelonnette for estimation of economic impact on the physical elements at risk in the area. In: Malet JP, Glade T, Casagli N (eds) Mountain risks – bringing science to society. CERG, Strasbourg

Bhattacharya N, Alkema D, Kingma NC (2010b) Integrated flood modeling for hazard assessment of the Barcelonnette municipality, South French Alps. In: Malet JP, Glade T, Casagli N (eds) Mountain risks – bringing science to society. CERG, Strasbourg

Blahut J (2009) Debris flow hazard and risk analysis at medium and local scale. PhD dissertation. University of Milan Bicocca, Faculty of Mathematical, Physical and Natural Sciences. Department of Environmental and Territorial Sciences, pp230

Buck W, Merkel U (1999) Auswertung der HOWAS – Datenbank, Institut fur Wasserwirtschaft und Kulturtechnik (IWK) der Universitat Karlsruhe, Karlsruhe, Report Nr. HY 98/15

Buriks C, Bohn W, Kennett M, Scola L, Srdanovic B (2004) Using HAZUS-MH for risk assessment: how-to guide. Technical Report 433, FEMA

Cannon S, DeGraff J (2009) The increasing wildfire and post-fire debris-flow threat in western USA, and implications for consequences of climate change. In: Sassa K, Canuti P (eds) Landslides – disaster risk reduction. Springer, Heidelberg

CAPRA (2012) Central American Probabilistic Risk Assessment (CAPRA). World Bank. www.ecapra.org

Carboni R, Catani F, Iotti A, Monti L (2002) The Marano landslide (Gaggio Montano, Appennino Bolognese) of February 1996. Quaderni Geol Appl 8(1):123–136

Carpignano A, Golia E, Di Mauro C, Bouchon S, Nordvik J-P (2009) A methodological approach for the definition of multi-risk maps at regional level: first application. J Risk Res 12:513–534

Cassidy MJ, Uzielli M, Lacasse S (2008) Probability risk assessment of landslides: a case study at Finneidfjord. Can Geotech J 45:1250–1267

Cepeda J, Díaz MR, Nadim F, Høeg K, Elverhøi A (2009) An empirical threshold model for rainfall-induced landslides: application to the Metropolitan Area of San Salvador, El Salvador

Corominas J (1996) The angle of reach as a mobility index for small and large landslides. Can Geotech J 33:260–271

Corominas J, Copons R, Vilaplana J, Altimir J, Amigó J (2003) Integrated landslide susceptibility analysis and hazard assessment in the principality of Andorra. Nat Hazards 30:421–435

de Pippo T, Donadio C, Pennetta M, Petrosino C, Terlizzi F, Valente A (2008) Coastal hazard assessment and mapping in Northern Campania, Italy. Geomorphology 97:451–466

Delmonaco G, Margottini C, Spizzichino D (2006a) ARMONIA methodology for multi-risk assessment and the harmonisation of different natural risk maps. Deliverable 3.1.1, ARMONIA
Delmonaco G, Margottini C, Spizzichino D (2006b) Report on new methodology for multi-risk assessment and the harmonisation of different natural risk maps. Deliverable 3.1, ARMONIA
Durham K (2003) Treating the risks in cairns. Nat Hazards 30(2):251–261
Egidi D, Foraboschi FP, Spadoni G, Amendola A (1995) The ARIPAR project: analysis of the major accident risks connected with industrial and transportation activities in the Ravenna area. Reliab Eng Syst Safe 49(1):75–89
Egli T (1996) Hochwasserschutz und Raumplanung. Schutz vor Naturgefahren mit Instrumenten der Raumplanung – dargestellt am Beispiel von Hochwasser und Murgängen. vdf Hochschulverlag AG, ETH Zürich
European Commission (2011) Risk assessment and mapping guidelines for disaster management. Commission staff working paper, European Union
FEMA (2004) HAZUS-MH. FEMA's methodology for estimating potential losses from disasters. US Federal Emergency Management Agency. http://www.fema.gov/plan/prevent/hazus/index.shtm
Flageollet JC, Maquaire O, Martin B, Weber D (1999) Landslides and climatic conditions in the Barcelonnette and Vars basins (Southern French Alps, France). Geomorphology 30(1–2):65–78
Fuchs S, Heiss K, Hóbl J (2007) Towards an empirical vulnerability function for use in debris flow risk assessment. Nat Hazard Earth Syst 7:495–506
Geomer (2008) FloodArea – ArcGIS extension for calculating flooded areas: user manual. Geomer GmbH and Ingenieurgemeinschaft
Greiving S, Fleischhauer M, Lückenkötter J (2006) A methodology for an integrated risk assessment of spatially relevant hazards. J Environ Plann Man 49(1):1–19
Grossi P, Kunreuther H, Patel CC (2005) Catastrophe modeling: a new approach to managing risk. Springer, New York
Grünthal G, Thieken AH, Schwarz J, Radtke KS, Smolka A, Merz B (2006) Comparative risk assessments for the City of Cologne – storms, floods, earthquakes. Nat Hazards 38(1–2):21–44
Guzzetti F, Peruccacci S, Rossi M, Stark CP (2008) The rainfall intensity-duration control of shallow landslides and debris flows: an update. Landslides 5(1):3–17
Hollenstein K (2005) Reconsidering the risk assessment concept: standardizing the impact description as a building block for vulnerability assessment. Nat Hazard Earth Syst 5:301–307
Horton P, Jaboyedoff M, Bardou E (2008) Debris flow susceptibility mapping at a regional scale. In: 4th Canadian Conference on Geohazards, Québec, Canada. Université Laval
Hussin HY, Quan Luna B, van Westen CJ, Christen M, Malet JP, van Asch TWJ (2012) Parameterization of a numerical 2-D debris flow model with entrainment: a case study of the Faucon catchment, Southern French Alps. Nat Haz Earth Syst Sci (NHESS) 12(10):3075–3090
Jones T, Middelmann M, Corby N (2005) Natural hazard risk in Perth, Western Australia. The cities project, Geosci Aus. http://www.ga.gov.au/hazards/reports/perth/
Kappes M, Glade T (2011) Landslides considered in a multi-hazard context. In: Proceedings of the second world landslide forum, Rome
Kappes M, Keiler M, Glade T (2010) From single– to multi-hazard risk analyses: a concept addressing emerging challenges. In: Malet JP, Glade T, Casagli N (eds) Mountain risks – bringing science to society. CERG, Strasbourg
Kappes MS, Malet JP, Remaitre A, Horton P, Jaboyedoff M, Bell R (2011) Assessment of debris-flow susceptibility at medium-scale in the Barcelonnette Basin, France. Nat Hazard Earth Syst 11:627–641
Kappes M, Gruber KSF, Bell R, Keiler M, Glade T (2012a) A medium/regional-scale multi-hazard risk analysis tool: the multirisk platform. Geomorphology 151–152:139–155
Kappes M, Gruber K, Glade T (2012b) Multi-hazard risk analyses with MultiRISK – tools for a user-friendly performance. In: 12th congress INTERPRAEVENT, Grenoble

Lacasse S, Eidsvik U, Nadim F, Hoeg K, Blikra LH (2008) Event tree analysis of Aknes rock slide hazard. In: Locat J, Perret D, Turmel D, Demers D, Leroueil S (eds) Proceedings of the IVth Canadian conference on geohazards: from causes to management. Presse de l'Université Laval, Québec, pp 551–557

Lecarpentier MC (1963) La Crue de Juin 1957 en Ubaye et ses consequences morphodynamiques. PhD dissertation, University of Strasbourg

Lee K, Rosowsky D (2006) Fragility analysis of woodframe buildings considering combined snow and earthquake loading. Struct Safe 28:289–303

Luino F (2005) Sequence of instability processes triggered by heavy rainfall in the northern Italy. Geomorphology 66:13–39

Maggioni M (2004) Avalanche release areas and their influence on uncertainty in avalanche hazard mapping. PhD dissertation, Universität Zürich

Malet JP, Remaitre A (2011) Statistical and empirical models for prediction of precipitation-induced landslides. Barcelonnette case study. Safeland deliverable. EU Safeland project

Maquaire O, Malet JP, Remaître A, Locat J, Klotz S, Guillon J (2003) Instability conditions of marly hillslopes: towards landsliding or gullying? The case of the Barcelonnette basin, south east France. Eng Geol 70(1–2):109–130

Marzocchi W, Mastellone M, Di Ruocco A (2009) Principles of multi-risk assessment: interactions amongst natural and man-induced risks. European Commission

MATE/MATL (1999) Plan de prévention des risques (PPR): risques de mouvements de terrain, ministère de l'Aménagement du territoire et de l'Environnement (MATE), ministère de l'Equipement des transports et du logement (METL). La Documentation Française, Paris, 72p

Molina S, Lang DH, Lindholm CD (2010) SELENA – an open-source tool for seismic risk and loss assessment using a logic tree computation procedure. Comput Geosci 36(3):257–269

Montgomery D, Dietrich W (1994) A physically based model for the topographic control on shallow landsliding. Water Resour Res 30:1153–1171

OMIV – Barcelonnette area. http://eost.u-strasbg.fr/omiv/data.php. Accessed Apr 2013

Penning-Rowsell EC, Johnson C, Tunstall S, Morris J, Chatterton J, Cokera A, Green C (2003) The benefits of flood and coastal defence techniques and data for 2003. Flood hazard Research Centre, Middlesex University, Middlesex

Perles Roselló M, Cantarero Prados F (2010) Problems and challenges in analyzing multiple territorial risks: methodological proposals for multi-hazard mapping. Boletín de la Asociación de Geógrafos Espanoles 52:399–404

Quan Luna B, Blahut J, van Westen CJ, Sterlacchini S, van Asch TWJ, Akbas SO (2011) The application of numerical debris flow modelling for the generation of physical vulnerability curves. Nat Hazard Earth Syst 11:2047–2060

RADIUS (1999) RADIUS method (Risk Assessment Tools for Diagnosis of Urban Areas against Seismic Disasters). http://www.geohaz.org/news/images/publications/RADIUS_RiskAssessment.pdf

Ramesh A, Glade T, Alkema D, Krol BGCM, Malet JP (2010) Model performance analysis for flood hazard assessment in Ubaye river, Barcelonnette, France. In: Malet JP, Glade T, Casagli N (eds) Mountain risks – bringing science to society. CERG, Strasbourg

Reese S, Bell R, King A (2007) RiskScape: a new tool for comparing risk from natural hazards. Water Atmos 15:24–25

Remaître A (2006) Morphologie et dynamique des laves torrentielles : application aux torrents des Terres Noires du bassin de Barcelonnette (Alpes du Sud). PhD dissertation, University of Caen Basse-Normandie, Caen

Remondo J, Bonachea J, Cendrero A (2008) Quantitative landslide risk assessment and mapping on the basis of recent occurrences. Geomorphology 94:496–507

Sarker JK, Ansary MA, Rahman MS, Safiullah MM (2010) Seismic hazard assessment for Mymensingh, Bangladesh. Environ Earth Sci 60:643–653

Schmidt J, Matcham I, Reese S, King A, Bell R, Henderson R, Smart G, Cousins J, Smith W, Heron D (2011) Quantitative multi-risk analysis for natural hazards: a framework for multi-risk modeling. Nat Hazards 58(3):1169–1192

Sedan O, Mirgon C (2003) Application ARMAGEDOM Notice utilisateur, BRGM open file BRGM/RP-52759-FR

Shi P (2002) Theory on disaster science and disaster dynamics. J Natural Disaster 11:1–9

Shi P, Shuai J, Chen W, Lu L (2010) Study on the risk assessment and risk transfer mode of large scale disasters. In: The 3rd international disaster and risk conference *IDRC*, Davos

Sirangelo B, Versace P (2002) Un modello probabilistico per la predizione in tempo reale delle altezze di precipitazione a scala oraria. Proceedings 'XXVIII Convegno di Idraulica e Costruzioni Idrauliche', Potenza, 2:395–414

Smith K, Petley DN (2008) Environmental hazards. Assessing risk and reducing disaster. Taylor & Francis, London

Spadoni G, Egidi D, Contini S (2000) Through ARIPAR-GIS the quantified area risk analysis supports land-use planning activities. J Hazard Mater 71(1–3):423–437

Tarvainen T, Jarva J, Greiving S (2006) Spatial pattern of hazards and hazard interactions in Europe. In: Schmidt-Thomé P (ed) Natural and technological hazards and risks affecting the spatial development of European regions. Geological survey of Finland, special paper 42. Geological Survey of Finland, Espoo, pp 83–91, 2 tables, 3 maps

Thiery Y, Malet J-P, Maquaire O (2006) Test of Fuzzy logic rules for landslide susceptibility assessment. In: Weber C, Gancarski P (eds) SAGEO 2006, Proceedings international conference on spatial analysis and geomatics, Strasbourg, France, CD-Rom Support Proceedings, 18 p

Thiery Y, Malet JP, Sterlacchini S, Puissant A, Maquaire O (2007) Landslide susceptibility assessment by bivariate methods at large scales: application to a complex mountainous environment. Geomorphology 9(1–2):8–59

Thierry P, Stieltjes L, Kouokam E, Nguéya P, Salley PM (2008) Multi-hazard risk mapping and assessment on an active volcano: the GRINP project at Mount Cameroon. Nat Haz 45:429–456

Van Westen CJ (2009) Multi-hazard risk assessment, guide book. Distance education course, Faculty of Geo-Information Science and Earth Observation (ITC), University of Twente

Van Westen CJ (2010) GIS for the assessment of risk from geomorphological hazards. In: Geomorphological hazards and disaster prevention. Cambridge University Press, Cambridge

Van Westen CJ, Montoya L, Boerhoom L, Coto EB (2002) Multi-hazard Risk Assessment using GIS in Urban areas: a case study for the city of Turrialba, Costa Rica. Proceedings of Regional Workshop on Best Practices in Disaster Mitigation, Lessons learned from the Asian Urban Disaster Mitigation Program and other initiatives, 24–26 September, Bali, pp 53–72

Van Westen CJ, Castellanos Abella, E.A. and Sekhar, L.K. (2008) Spatial data for landslide susceptibility, hazards and vulnerability assessment: an overview. Eng Geol 102(3–4):112–131

Van Westen CJ, Castellanos Abella EA, Sekhar LK (2008) Spatial data for landslide susceptibility, hazards and vulnerability assessment: an overview. Eng Geol 102 (3–4):112–131

Varnes DJ (1984) Landslide hazard zonation: a review of principles and practice. Commission on landslides of the IAEG, UNESCO. Nat Hazards 3:61

Yeh CH, Loh CH, Tsai KC (2006) Overview of Taiwan earthquake loss estimation system. Nat Hazards 37(1–2):23–37

Young OR (2002) The institutional dimension of environmental change: fit, interplay, and scale. MIT Press, Cambridge

Young OR (2003) Environmental governance: the role of institutions in causing and confronting environmental problems. Int Environ Agreements Polit Law Econ 3(4):377–393

Zêzere JL, Garcia RAC, Oliveira SC, Reis E (2008) Probabilistic landslide risk analysis considering direct costs in the area north of Lisbon (Portugal). Geomorphology 94:467–495

Zuccaro G, Leone M (2011) Volcanic crisis management and mitigation strategies: a multi-risk framework case study. Earthzine 4